



# Engineering Lightweight Aluminum and Magnesium Alloys for a Sustainable Future

Payam Emadi, Bernoulli Andilab and C. Ravindran\*

**Abstract** | Lightweight alloys such as magnesium and aluminum have been garnering increasing interest due to the global demand for emission reduction and sustainability. Such alloys are excellent candidates for replacing high-density iron-based materials, leading to weight reduction and associated improvements in energy consumption. In addition, alloys with improved thermal properties such as thermal conductivity can aid in electric vehicle operation and internal combustion engine efficiency. However, to further promote the use of lightweight materials in industry, their mechanical and thermal properties must be enhanced, especially for magnesium alloys. To this end, this article summarizes recent progress toward improving the properties of cast magnesium and aluminum alloys in the fields of grain refinement using potent nucleants and solutes, thermal conductivity enhancement through microstructure modification and heat treatment, magnesium melt cleanliness assessment and control as well as ultrasonic assisted casting of light alloys. The current state of literature illustrates tremendous strides toward magnesium and aluminum alloys with high strength and improved thermal properties. Such materials will be invaluable for addressing the current and future challenges of sustainability, environment and energy.

## 1 Introduction

With the ever-increasing crisis of CHG emissions, global warming and climate change, researchers from across the globe have been focusing their efforts on lightweight and high-strength alloys. Their goal is to substitute high-density materials such as steel with lightweight alloys and metal matrix composite materials. However, despite the necessity to develop towards net zero global emissions and a sustainable future, anthropogenic carbon emissions are constantly rising<sup>1</sup>.

From a light weighting perspective, high-specific strength alloys such as magnesium (Mg) or aluminum (Al) are excellent candidates. Magnesium alloys can be approximately 70% lighter than steel and 30% lighter than Al<sup>2</sup>. However, despite the advantages of using Al and Mg alloys for light weighting, they are not as prevalent as iron-based alloys. This is primarily due to their lower mechanical properties such as

tensile strength, ductility, and creep resistance<sup>2</sup>. As a result, to promote the enhanced use of lightweight alloys in the transportation, aerospace and electronics industry, their mechanical properties must be improved. This is especially critical for applications where load bearing capacity is a concern.

Researchers have been seeking alternative methods for improving the properties of light alloys for numerous years. As a result of extensive research, grain refinement has been identified as an effective method<sup>3</sup>. **Grain refinement** can simultaneously improve the strength and ductility of alloys<sup>4</sup>. Moreover, it aids in reducing casting defects such as segregation. Grain refinement can also improve the formability of wrought alloys by eliminating their columnar structure. Therefore, grain refinement is an effective technique for improving the properties of light alloys, enabling their increased use in industry.

**Grain refinement:** A method for enhancing the quality of castings by increasing grain boundary area and homogenizing the microstructure.

<sup>1</sup> Centre for Near-Net-Shape Processing of Materials, Ryerson University, 350 Victoria Street, Toronto, ON M5B 2K3, Canada.  
\*rravindr@ryerson.ca

In addition to improving mechanical properties, thermal properties of alloys must also be improved. This is particularly important for internal combustion (IC) engines and electric vehicles (EV). In conventional IC engines, engine components that operate at elevated temperatures, such as engine blocks and cylinder heads, must efficiently dissipate heat. If the heat is not adequately dissipated, thermo-mechanical stresses from uneven expansion can lead to reduced engine efficiency and decreased component life. Heat dissipation is also important for EVs. For example, heat is generated from batteries and electric motors that must be dissipated through their housing components. This is especially true for lithium-ion-based batteries that generate a sizable amount of heat, which is typically uneven throughout the components. Inadequate thermal management can diminish the performance and life of the battery<sup>5</sup>. As a result, effective heat dissipation is critical for safe, efficient and reliable operation of EVs and a comprehensive understanding of factors that affect thermal conductivity of light alloys is essential.

**Heterogenous nucleation:** Initiation of nucleation from foreign substances in liquid metal.

**Ultrasonic processing:** The application of high-intensity ultrasonic vibration to liquid metal using a sonotrode.

Critical modern technologies such as **ultrasonic processing** are important for promoting the use of lightweight alloys. Ultrasonic irradiation is one such technology that has been used successfully in the refinement of Al alloys and also offers immense potential for Mg<sup>6-8</sup>. Ease of operation, potent grain refining capability, and low-cost equipment contribute to its capacity for industrial application. Since the viscosity of Mg melt is similar to that of water, it can be sonicated with comparatively low attenuation, enabling refinement of large melt volumes<sup>9,10</sup>. Additionally, melt contamination by oxidation is substantially diminished during irradiation, since the melt surface is left nearly undisturbed. However, the sonication technique is largely undeveloped and requires further investigation, especially in application to Mg alloys.

The purpose of this review is to describe various methods for improving the mechanical and thermal properties of lightweight alloys. Hence, the article has been divided into four parts: (1) grain refinement of magnesium alloys, (2) thermal conductivity of aluminum alloys, (3) magnesium melt cleanliness and (4) ultrasonic processing of lightweight alloys. The authors hope to promote a better understanding of fundamentals and novel approaches to improving light alloys. The need for this review emanates from the tremendous potential of light alloys in impacting and shaping our future. Researchers are continuously contributing to this global

**Lattice:** A repeating group of atoms arranged in a distinct pattern.

theme. However, the quest for developing novel materials that can address the challenges of environment, energy and sustainability is an on-going phenomenon.

## 2 Grain Refinement of Magnesium Alloys

Grain refinement is a critical method for improving the strength of cast alloys. Grain refinement can be effected through several processes and this article will focus on two predominant views. First, is grain refinement through **heterogenous nucleation**. This typically involves the addition of potent nucleants to act as substrates for the formation of new grains. The second approach is grain refinement through solute segregation, which operates through restricting the growth of grains, leaving more time for new grains to form and grow. Moreover, a solute-induced constitutional supercooling area formed ahead of the solidification front can trigger the formation of new grains, which can further restrict grain growth. In either case, the effectiveness of grain refinement methods can be established through the magnitude of undercooling prior to solidification. In effect, the lower the undercooling, the higher the potency of the grain refiner. Within the past years, a great number of elements and compounds have been evaluated for their grain refinement capability in Mg alloys. In this section, several of the more recent research in this field will be presented, followed by a future outlook.

### 2.1 Heterogeneous Nucleation from Particle Substrates

Grain refinement through particle addition is an effective method of refining alloy grain size. Selection of a suitable particle or refiner is extremely critical. Nucleating particles must have a higher melting point than the liquid metal and be stable at elevated temperatures<sup>11</sup>. This is crucial to avoid dissolution of the refiner particles or any undesired chemical reactions between the particles and the liquid metal. Grain refiner particles should also have a density that is near that of the liquid metal<sup>12,13</sup>. If the density of the particles is higher than the melt, we risk fast settling of the refiner particles. In contrast, if the density is lower, the particles may float to the top of the melt where they can be skimmed away. In either case, the grain refining potential is significantly reduced. Finally, to minimize the energy required for effective nucleation, the particles and the host metal should have high crystallographic registry. Several methods have been proposed to evaluate **lattice** matching such as the

**Table 1:** Planar disregistry values for select substrates in Mg.

Substrate	Planar Disregistry (%)	Source
Mg	–	–
Zr	<0.5	17
SiC	2.3	18
Al <sub>4</sub> C <sub>3</sub>	3.35	19
Al <sub>2</sub> CO	1.21	20
Al <sub>2</sub> MgC <sub>2</sub>	5.32	21
AlCMn <sub>3</sub>	15	22
AlB <sub>2</sub>	6.09	23
Al <sub>3</sub> BC	8.8	24
TiB <sub>2</sub>	5.6	25
TiC	4.6	26
TiAl <sub>3</sub>	11.9	26
AlN	3.05	27

planar disregistry model proposed by Bramfitt<sup>14</sup> or the edge-to-edge matching model<sup>15</sup>. A summary of planar disregistries for select substrates can be seen in Table 1.

Magnesium alloys can be divided into two systems, Mg–Al alloys and Mg alloys free of Al. For Mg alloys that do not contain Al, zirconium (Zr) has been identified as a highly effective refiner. Researchers have reported that minor additions of Zr can reduce the average grain size up to 80%<sup>16</sup>. However, Zr addition is not suitable for alloys of Mg that contain other alloying elements such as Al, Mn or Si. This is primarily due to Zr forming stable compounds with the aforementioned elements, thereby decreasing its potential as a nucleating agent. Therefore, the search for a potent nucleant for the more popular Mg–Al alloy system is still on-going.

**Carbon inoculation** is perhaps one of the most widely researched areas for the grain

refinement of Mg. Carbon is typically introduced to the liquid metal in the form of chemical compounds such as C<sub>2</sub>Cl<sub>6</sub>, allotropes of carbon such as graphite powder or carbonaceous gasses such as CO<sub>2</sub> or CO<sup>28–32</sup>. Several theories exist to explain the cause for refinement with the addition of carbon. The most widely accepted theory is the formation of Al<sub>4</sub>C<sub>3</sub> during the casting process. Based on the disregistry models explained previously, researchers have found that Al<sub>4</sub>C<sub>3</sub> can indeed act as a potent nucleant for Mg<sup>16,29</sup>. Other carbon-containing **intermetallic compounds** have also been suggested as potential sources for Mg nucleation, such as Al<sub>2</sub>MgC<sub>2</sub> and Al<sub>2</sub>CO; however, further research is required to fully validate these claims<sup>28,32</sup>.

Recently, Tong et al.<sup>33</sup>, examined the effect of C<sub>2</sub>H<sub>2</sub> as a novel carbon-based gas inoculant on an **AM60B** magnesium alloy. The researchers also compared the effectiveness of the novel gas to the more conventional CO<sub>2</sub> gas inoculation method. The experimental procedure consisted of melting the AM60 alloy at 760 °C and bubbling either C<sub>2</sub>H<sub>2</sub> or CO<sub>2</sub> gas for 10, 20, 30, 60 and 120 min. As seen in Fig. 1a and b, the finest grain size for the C<sub>2</sub>H<sub>2</sub> refined alloys was achieved by bubbling for 30 min, which reduced the average grain size from 412 to 101 μm. As well, a significant improvement in YS, UTS and %Elongation was observed from 77 MPa, 147 MPa, and 5.73% for the base alloy to 92 MPa, 201 MPa, and 8.14%, respectively. When compared to CO<sub>2</sub> (Fig. 1c), the finest grain size was achieved at bubbling for 10 min, which reduced the grain size to 92 μm. The YS, UTS and %Elongation were 89 MPa, 188 MPa and 7.03%, respectively. In both cases, the refinement was attributed to heterogenous nucleation from Al<sub>4</sub>C<sub>3</sub> particles formed during the bubbling stage. The authors determined that although bubbling with CO<sub>2</sub> led to a finer grain size, the mechanical properties of the casting refined with C<sub>2</sub>H<sub>2</sub> were higher. This was thought to have been caused by the

**Intermetallic compound:**

Solid phases that consist of two or more metallic or semi-metallic elements and an ordered structure.

**AM60B:** An alloy of magnesium containing 6.0% aluminum and 0.13% manganese, by weight.

**Carbon inoculation:** Addition of carbon-based compounds to the liquid metal for the purpose of grain refinement.

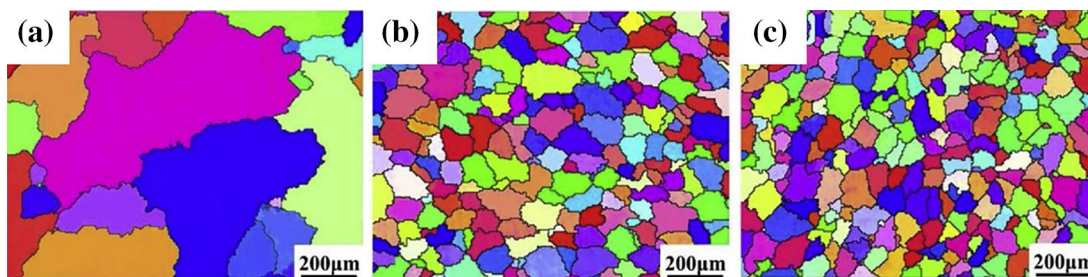


**Figure 1:** EBSD of AM60 alloys **a** base alloy, **b** alloy treated with C<sub>2</sub>H<sub>2</sub> for 30 min and **c** alloy treated with CO<sub>2</sub> for 10 min<sup>34</sup>.

formation of impurities, MgO and MgAl<sub>2</sub>O<sub>4</sub>, as a result of CO<sub>2</sub> bubbling.

Another widely used method to refine Mg alloys is the use of borides such as TiB<sub>2</sub>, ZrB<sub>2</sub> and MgB<sub>2</sub><sup>35–38</sup>. A recent study performed by Sahoo et al.<sup>37</sup>, investigated the use of in situ-formed TiB<sub>2</sub> particles on the microstructure and mechanical properties of ZE41 Mg alloy. The researchers used a novel grain refiner preparation method that utilized ball milling of Ti and B particles with a ratio of 68:32 (stoichiometry of TiB<sub>2</sub>). Subsequently, the milled powder was melted together with the ZE41 alloy at 900 °C to prompt the in situ reaction, forming TiB<sub>2</sub>. Sahoo et al.<sup>37</sup> reported a reduction in grain size from 95.25 μm in the base alloy to 32.21 μm in the alloy with 15 wt% TiB<sub>2</sub>. However, the mechanical properties at 15 wt% TiB<sub>2</sub> were compromised due to grain refiner agglomeration. The optimal mechanical properties were achieved at the 10 wt% TiB<sub>2</sub> addition level, which resulted in an improvement in YS, UTS and %Elongation of 138%, 113% and 5.3%, respectively. As a result, TiB<sub>2</sub> was highly effective in enhancing the grain size and mechanical properties of ZE41.

Researchers have also examined the grain refining potential of nitrides such as AlN, BN or VN on Mg alloys<sup>39–41</sup>. Qiu et al.<sup>40</sup> recently investigated the effects of VN addition on the grain refinement and mechanical properties of AZ31 Mg alloy. The experimental procedure consisted of the addition of 0.5, 1, and 2 wt% of 1 μm VN powder and stirring for 15 min. The researchers reported that the 0.5 wt% addition level led to the highest level of refinement. The grain size was reduced from 115.7 to 62.4 μm. Moreover, the YS, UTS and %Elongation improved from 39.5 MPa, 140.7 MPa and 10.6% to 47.1 MPa, 197.4 MPa and 17.8% in the refined alloy. Qiu et al. attributed the improvement in properties to a duplex nucleation mechanism from VN and AlN. The AlN was suggested to have been formed through an in situ reaction between VN and Al during casting.

In addition to the traditional micro-particle additions, grain refinement using nano-sized particles has shown excellent promise in the refinement of cast Mg alloys<sup>42</sup>. Researchers have developed high-strength Mg matrix nano-composites with tensile properties that parallel that of mild steel. For example, Zhu et al. reported yield and tensile strengths of 424 MPa and 437 MPa for a Mg alloy prepared through the addition of TiC nanoparticles<sup>43</sup>. However, effective and homogeneous distribution of nanoparticles in the metal matrix is challenging. This is due to

the high specific surface area and consequent low wettability between the nanoparticles and the liquid metal<sup>44</sup>. Moreover, the application of conventional casting techniques such as stir casting typically results in particle agglomeration, which leads to poor mechanical properties. As a result, more complex casting technologies, such as ultrasonic processing, are required to effectively prepare nano-particle-reinforced Mg castings.

In summary, grain refinement achieved through either micro- or nano-particle addition is effective in improving the mechanical properties of cast Mg alloys. Several particles and nucleating substrates have been proposed and experimented with, all with varying success. Crystallographic models such as the Bramfitt model have shown relatively good success in determining effective nucleants. However, it is clear that further research is required to identify a nucleant as potent as Zr for Al-free Mg alloys.

## 2.2 Solute Addition

Solute addition is a particularly important method to refine the grains of alloys. This is primarily due to solute rejection at the solid/liquid interface and the consequent constitutional undercooling. The grain refining efficiency of a particular alloying element can be quantified using the Growth Restriction Factor (GRF) or  $Q$  as described with Eq. (1) below<sup>45</sup>:

$$Q = mC_0(k - 1), \quad (1)$$

where  $m$  is the slope of the liquidus line,  $C_0$  is the initial composition of the alloy, and  $k$  is the equilibrium partition coefficient for the element. The GRF quantifies the ability of elements to segregate during solidification, with higher values leading to better refinement. Table 2 presents a summary of GRF values for several common elements used for Mg alloys. However, it must be noted that the GRF does not consider the solubility of an element in the host metal. In effect, elements with limited solubility are less likely to refine grains by grain growth restriction.

Of the typical alloying elements for Mg alloys, Al has proven to be highly effective in refining the microstructure and mechanical properties. Aluminum is known to widen the freezing range of Mg alloys, thereby facilitating easier casting<sup>2</sup>. Zinc (Zn) is also known to be a highly effective alloying element for Mg alloys. Typically, Zn and Al are added together to improve room-temperature strength<sup>2</sup>. The addition of rare earth metals can improve elevated temperature mechanical properties<sup>2</sup>. In addition, Si can be used to increase

**ZE41:** An alloy of magnesium containing 4.2% zinc, 0.7% Zr and 1.2% rare earth elements, by weight.

**Solute rejection:** Decrease of solute content in solidifying metal due to changes in solubility limit.

**AZ31:** An alloy of magnesium containing 3.0% aluminum, 0.2% manganese and 1.0% zinc, by weight.

**Constitutional undercooling:** Supercooling of liquid metal that occurs due to changes in composition.

**Freezing range:** The range of temperature between the solidus and liquidus of an alloy.

**Table 2:** GRF or Q values for solute elements at 1 wt%<sup>46</sup>.

Element	$m(K-1)$ reported in <sup>47</sup>	$m(K-1)$ reported in <sup>3</sup>
Fe	52.68	52.56
Zr	30.24	38.29
Ca	8.786	11.94
Si	9.42	9.25
Ni	6.053	6.13
Zn	5.003	5.31
Cu	7.402	5.28
Ge	4.778	4.41
Al	4.26	4.32
Sr	3.474	3.51
Ce	2.749	2.74
Sc	2.058	2.61
Yb	2.68	2.53
Y	1.624	1.7
Sn	1.446	1.47
Pb	1.002	1.03
Sb	0.69	0.53
Mn	0.038	0.15
Ti <sup>48</sup>	-	59,500

fluidity and Mn addition aids in the removal of iron and other heavy elements during casting<sup>2</sup>.

Researchers Joshi and Babu<sup>49</sup> examined the effect of bismuth (Bi) addition to pure Mg. The GRF for Bi in Mg at 1.0 wt% has been reported to be 1.55<sup>47</sup>. The researchers experimented with 0.02, 0.04, 0.08, 0.1 and 0.4 wt% Bi addition levels. Joshi and Babu<sup>49</sup> reported excellent grain refining efficiency for Bi, with 0.4 wt% leading to the highest refinement. At this addition level, the

grain size reduced from 1200  $\mu\text{m}$  in the base alloy to 400  $\mu\text{m}$  (Fig. 2). The researchers identified Mg–Bi–O-based secondary phases in the alloy matrix, which were thought to have been potent nucleation sites for Mg. A similar study performed by Guangyin et al.<sup>50</sup> also examined the effect of Bi in an AZ91 Mg alloy. The researchers reported the highest YS and UTS at 2 wt% Bi which improved from 106 and 222 MPa to 184 MPa and 265 MPa, respectively. The researchers reported the formation of an  $\text{Mg}_3\text{Bi}_2$  phase in the microstructure. The newly formed phase was said to have superior elevated temperature stability, leading to improved high-temperature mechanical properties and creep resistance. As a result, Bi is clearly a potent grain refiner for Mg alloys. However, the refinement effect is not purely solute related, but nucleation through Mg–Bi-based phases such as  $\text{Mg}_3\text{Bi}_2$  have also been reported<sup>49</sup>.

Samarium (Sm) addition has also been gaining some interest as of late. The GRF of Sm has been reported as 2.94 at 1.0 wt% addition<sup>47</sup>. Zhang et al.<sup>51</sup> examined the effect of Sm addition on the microstructure and mechanical properties of a Mg–6Zn–0.4Zr alloy. Addition levels of 0, 2, 4 and 6 wt% were investigated. The researchers reported that Sm addition resulted in the formation of  $\text{Mg}_{41}\text{Sm}_5$  and  $\text{MgZnSm}$  phases. With increasing Sm content from 0 to 6%, the transformation of the eutectic phase morphology from an isolated island to a completely continuous network form was observed. When larger addition levels of Sm ( $\geq 4$  wt%) was used, perfect lamellar eutectic microstructures were formed. Additionally, the grain size of the alloys decreased with increasing Sm content up to 2 wt%, whereafter the grain size coarsened. Quantitative values for grain size were not reported. Samarium addition also influenced the tensile properties of the

**Creep:** Time dependent deformation under persistent stress that can cause a material to deform without reaching the yield limit. Typically occurs at elevated temperatures.

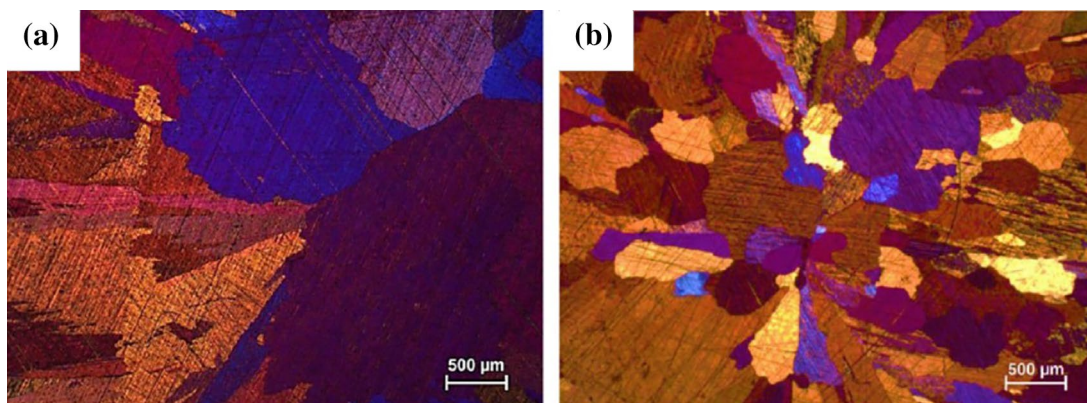


**Figure 2:** Optical micrograph of **a** base alloy and **b** Mg + 0.4 wt% Bi<sup>49</sup>.

**IACS:** International Annealed Copper Standard, established by the 1913 International Electrochemical Commission. The conductivity of annealed copper is defined as 100% IACS at 20 °C, which is used as a reference for other conductivity values.

alloys. Zhang et al.<sup>51</sup>, reported improvements in UTS and %Elongation from 184 MPa and 6.02% in the base alloy to 214 MPa and 7.42% with the addition of 2 wt% Sm. Further increasing the Sm addition level did not improve the mechanical properties, which was said to be related to the MgZnSm phase and the morphology of eutectic phases.

To conclude, it is evident that research in the field of enhancing Mg alloys has gained significant ground in the recent years. However, it must be noted that grain refinement is a complex subject. Several theoretical models such as the grain growth restriction factor and disregistry models have been proposed, all with varying success. To achieve superior mechanical properties, researchers must explore solutions combining both the particle substrate and the solute effect paradigms. In effect, combinations of effective solutes to prompt constitutional undercooling as well as potent inoculant particles for heterogenous nucleation can lead to high-strength Mg alloys for use in industry.

### 3 Thermal Conductivity of Aluminum Alloys

Thermal conductivity is a property that describes the ability of a material to transfer heat internally, from a high- to low-temperature region. Conduction through a material occurs via lattice vibration waves and free electrons, which act as thermal energy carriers. Lattice vibrations involve the propagation of **phonons** through a material with a temperature gradient from high to low temperature. Subsequently, thermal energy can be converted into kinetic energy by free electrons. Therefore, an increase in kinetic energy of free electrons promotes more efficient flow through the temperature gradient of a material. In this section, an overview of studies on a range of factors that affect the thermal conductivity of Al alloys is discussed.

#### 3.1 Effect of Alloying and Microstructure

Aluminum alloys are less conductive compared to pure Al. This is due to the presence of impurities or alloying elements which act as scattering sites for thermal energy carriers, resulting in reduced conductivity. Depending on the solubility limit of alloying elements, they can be in solution or precipitate as a secondary phase. The concentration of alloying elements in solid solution, the volume fraction, size and morphology of secondary phases contribute to a reduction in thermal conductivity. Elements in solid solution

independently increase the resistivity of an alloy with increasing solute concentration. This was observed by Mulazimoglu et al.<sup>52</sup>, who determined that the electrical conductivity of Al–Si–Mg alloys decreased linearly with increasing Si or Mg concentrations. The decreases in conductivity were measured as 12% IACS per wt% Si and 10% IACS per wt% Mg. This was expected since both elements were dissolved into the Al matrix.

Secondary phases also reduce the thermal conductivity of an alloy, typically in proportion to the volume fraction of the phases present. Vandersluis et al.<sup>53</sup>, demonstrated the effect of Si morphology on electrical conductivity by modifying the eutectic Si in B319 Al alloy through Sr additions. It was found that the synergy between solidification rate and Sr addition directly corresponded to their combined roles in modifying the morphology of the eutectic Si particles. The results demonstrated that the electrical conductivity can improve from approximately 27–30% IACS with decreasing Si particle aspect ratio from approximately 2.4–1.5, decreasing circular diameter from approximately 10.0–0.8  $\mu\text{m}$ , or increasing sphericity from approximately 0.3–1.0. The smaller, rounder and less-elongated particles enabled more efficient electron transport through the material with greater mean free paths as compared to an unmodified Al–Si alloy<sup>53</sup>. The authors also noted that conductivity is diminished less by increasing amounts of eutectic Si phase in the matrix than by increasing amounts of Si in solid solution. Regardless of whether Si is present in the solution or in the eutectic phase, Mg reduces conductivity due to its dissolution. Therefore, the authors concluded that there was clear indication of the dominant role of the Si modification level on the conductivity of 319 alloy.

The effect of grain refinement or dendritic refinement on conductivity has also been studied. Vasquez Lopez et al.<sup>54</sup> demonstrated through casting by unidirectional solidification, that as the solidification rate increased along the casting, dendritic refinement was achieved. Subsequently, the increased refinement of dendrites corresponded to an increase in thermal conductivity. Other studies have also shown that dendritic refinement results in increased conductivity of Al alloys<sup>55,56</sup>. Conversely, while previous works determined that refinement by controlling cooling rate can result in increased conductivity, attention should be paid to the associated porosity formation during solidification. For example, slower solidification rates are likely to result in more porosity, thus reducing conductivity. Hence, the reduced conductivity may be attributed

**Phonon:** A phonon is a unit of vibrational mechanical energy formed from the oscillation of atoms in a crystal. The mechanical energy forms mechanical waves which can carry heat through a material.

**319:** An alloy of aluminum containing 6% silicon and 3.5% copper, by weight.

to porosity rather than coarser grains or dendrites and vice versa. This is further discussed in Sect. 3.3.

### 3.2 Effect of Heat Treatment

Heat treatment is an important part of Al alloy processing, which can enhance the as-cast properties for applications requiring higher performance. Following casting, the post-processing sequence typically begins with a solution heat treatment. For example, in Al–Si–Cu–Mg alloys, Cu- and Mg-rich particles are dissolved within the  $\alpha$ -Al lattice at a relatively elevated temperature. The alloy is then quenched to obtain an Al solid solution that is supersaturated with solute. Subsequently, artificial aging is carried out at intermediate temperatures to enable controlled precipitation of finely dispersed phases throughout the matrix. During the heat treatment process, a wide variety of material properties can be achieved by controlling the process parameters. Such parameters typically depend on alloy composition and casting prehistory<sup>57</sup>.

In addition to Cu dissolution during solution heat treatment, several other microstructural changes may occur during the high-temperature treatment of industrial Al alloys. Acicular eutectic Si particles in hypoeutectic Al–Si alloy systems are of particular importance. These phases have been found to fragment, spheroidize and coarsen during solution heat treatment<sup>58</sup>. The spheroidization and coarsening processes is known to occur more readily in alloys containing fibrous Al–Si eutectic structures, attained by prior chemical modification with trace Sr additions and/or increased solidification rates. Such modification of the microstructure, eutectic Si in particular, via heat treatment and Sr additions can lead to improvements in conductivity. This was demonstrated by Vandersluis et al.<sup>59</sup>, where the electrical conductivity of A319 Al alloy increased with increasing solution heat treatment time. The eutectic Si spheroidization and coarsening processes promoted subsequent conductivity increases by up to 10%, relative to the as-cast conditions (26.7–30.4% IACS). It was suggested that there were two competing processes that primarily affected conductivity: (1) dissolution of the Al<sub>2</sub>Cu phases and (2) spheroidization and coarsening of the Si phases.

**Age hardening** is a well-known method for improving mechanical properties. Recently, it has also been explored to improve the conductivity of Al alloys. It was found that artificial aging promoted significant changes in electrical

conductivity, demonstrated in Fig. 3. Castings were performed and poured in 500 and 200 °C moulds, while also subsequently adding strontium (Sr). The samples were then solution heat treated for 24, then age hardened at 250 °C. It was found that the 0Sr–500C, 0Sr–200C, 150Sr–500C and 150Sr–200C cast samples featured conductivities of approximately 33, 38, 35 and 38% IACS, respectively<sup>60</sup>. With increasing artificial aging time, conductivity was consistently and considerably enhanced. For each casting condition, this treatment promoted the highest electrical conductivity achieved in this study, corresponding to 25–30% improvements relative to their as-quenched values. While these maximum values in conductivity can be achieved, it should be noted that for practical applications, an optimal aging time should be selected to obtain both relatively high strength and conductivity.

### 3.3 Effect of Porosity

It is well known that casting **porosity** has a significant effect on the mechanical properties of a material, whether from shrinkage or gas. Additionally, porosity has been reported to decrease thermal conductivity, since it effectively impedes heat transfer. Manzano Ramirez et al.<sup>62</sup> introduced 0.43–10.35 vol% of gas porosity into a 380 Al alloy by increasing the liquid melt temperature to promote hydrogen dissolution. This resulted in the thermal conductivity decreasing linearly with increasing pore volume fraction. Similarly, this was also observed by Vandersluis et al.<sup>63</sup>, where increases in percentage porosity (~1–8%) resulted in a decrease in thermal conductivity (~130–80 W/mK). The results were also correlated with the cooling rate of the castings, where slower cooling resulted in increased porosity and consequently, a decrease in conductivity. Of note, this study also elucidated that refinement of secondary dendrite arm spacing (SDAS) via changes in cooling rate was not the main factor in changing conductivity. However, subsequent changes in cooling rate resulted in formation of pores, which in turn affected conductivity. That is to say, while decreasing cooling rate can increase the size of SDAS, it also results in increased interdendritic shrinkage porosity, which is detrimental to alloy conductivity.

In summary, thermal conductivity of Al alloys is influenced by metallurgical factors and microstructural features. This includes the solidification conditions and the resulting as-cast microstructure morphology, the addition of

**Porosity:** A casting defect characterized as a void in a cast material. Porosity can present itself as either gas or shrinkage porosity. The former arises from the dissolution of gases in the liquid melt, such as hydrogen in molten aluminum. The latter occurs during solidification when mass feeding compensates shrinkage as the liquid transforms from liquid to solid.

**Age hardening:** A heat treatment process utilized to enhance the mechanical properties of alloys by forming small nano-sized uniformly dispersed precipitates within the alloy matrix.

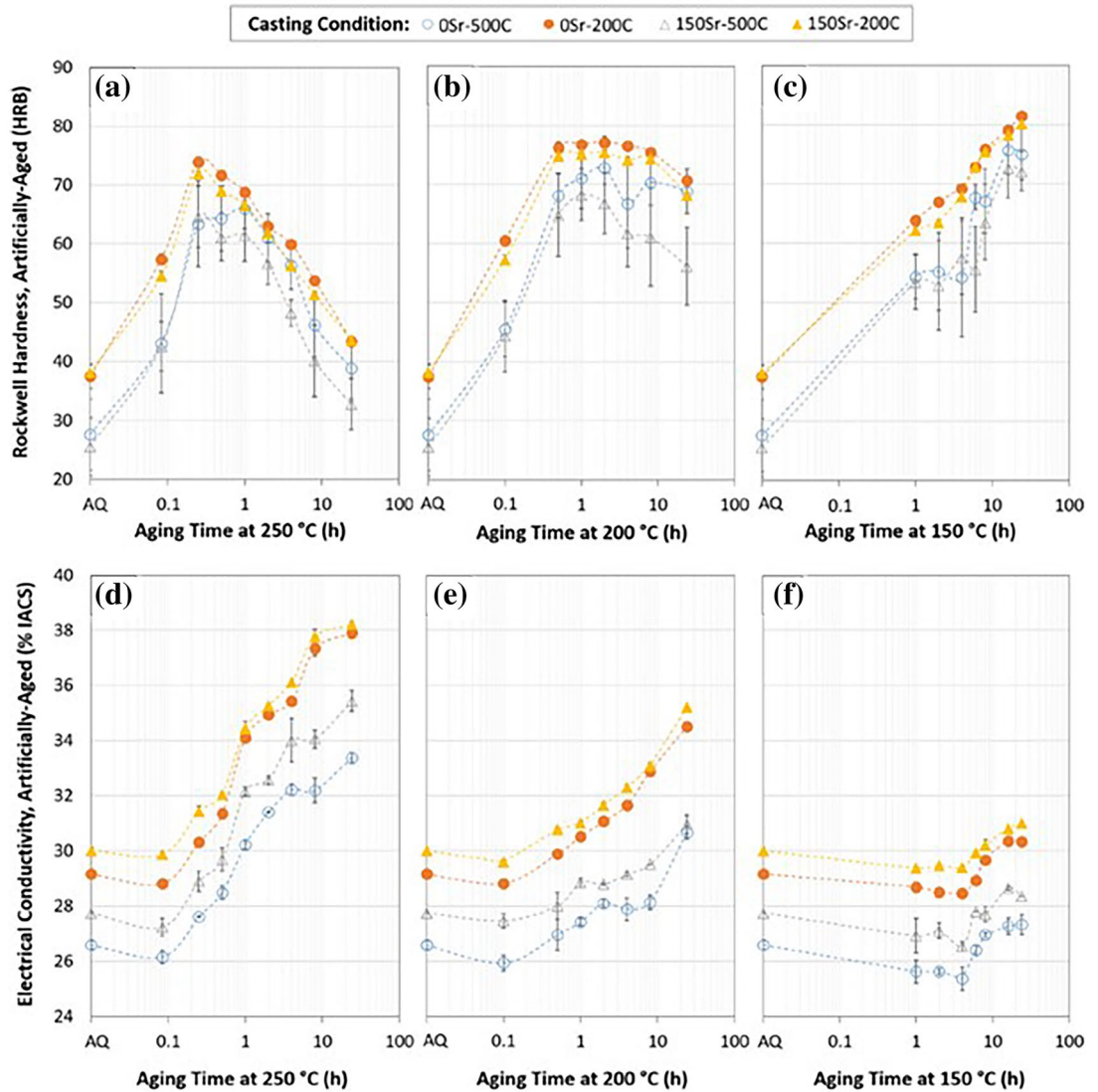


**Figure 3:** Ambient-temperature material properties of samples after precipitation heat treatment: Rockwell hardness after aging at **a** 250 °C, **b** 200 °C, and **c** 150 °C; electrical conductivity after aging at **d** 250 °C, **e** 200 °C, and **f** 150 °C. AQ—as-quenched following 24-h solution heat treatment at 500 °C<sup>41</sup>.

alloying elements, heat treatments, and porosity. Studies have shown that while thermal conductivity can easily be reduced due to the presence of scattering centers, there are methods which can be implemented to improve conductivity. This can be achieved through the modification of the microstructure by adding trace amounts of modifiers such as Sr or through heat treatment. The authors would like to note that the conductivity of Mg alloys has been extensively studied. The thermal conductivity of pure Mg (156 W/mK<sup>2</sup>) is significantly lower than that of pure Al (237 W/mK<sup>64</sup>). Extensive future research is necessary to elevate the conductivity of Mg alloys to the level of Al.

**Inclusion:** A defect characterized as a solid particle entrapped in a casting. During melting, inclusions typically form as a result of an oxidation reaction at elevated temperatures, such as magnesium oxide in magnesium castings.

#### 4 Magnesium Melt Cleanliness

With the push toward decreased greenhouse gas emissions and light weighting of vehicles, increased use of Mg alloys is becoming critical. Although Mg alloys have a higher specific strength when compared to Al and Fe-based alloys, their mechanical properties are not as high. This fact coupled with the high molten reactivity of Mg, is a barrier to its use in industry. Therefore, in addition to the methods mentioned previously to increase the strength of Mg alloys, particular attention must be paid to melt cleanliness. According to Lun Sin et al.<sup>65</sup>, a principal factor in ensuring melt cleanliness is control of unwanted inclusions. Inclusions in Mg alloys can

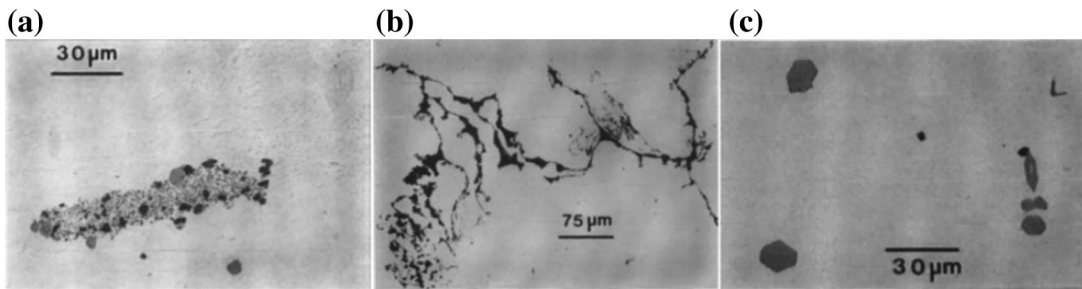


**Figure 4:** Optical micrographs of **a** oxide cluster in AZ91 alloy, **b** 'snaky' oxide in AM50 alloy and **c** Mn–Al particles in AM60 alloy<sup>63</sup>.

be divided into two groups, non-metallic inclusions such as oxides, nitrides and chlorides as well as intermetallic inclusions such as Fe-bearing phases<sup>66</sup>. Inclusions can be formed in many ways, some of the most common sources are reactions with air, reactions during the casting process and reactions with protective atmospheres or fluxes. Examples of three common inclusion types in Mg alloys can be seen in Fig. 4.

During the melting and casting process, molten Mg can readily react with oxygen in air to form magnesium oxide (MgO)<sup>66,67</sup>. Oxide inclusions can present themselves in many different **morphologies**, such as particles or films. Oxide films with high surface-to-volume ratios are particularly detrimental to mechanical properties since they cannot be removed by settling<sup>67</sup>. Magnesium can also react with the available nitrogen in air to form nitrides such as Mg<sub>3</sub>N<sub>2</sub>. However, it has been reported that Mg preferentially reacts with oxygen rather than nitrogen due to the lower Gibbs free energy for oxidation<sup>67</sup>. Molten Mg can also react with moisture in the air or on casting equipment to form MgO and hydrogen. Such an occurrence is dangerous since it could cause a fire or explosion. As a result, casting tools must be kept dry. Preheating tools prior to casting is an effective method for removing moisture.

Inclusions can form and become entrained during the casting process. For example, improper mold design can lead to turbulence during filling. Turbulent melt flow can entrain inclusions and expose a fresh melt surface to the atmosphere, leading to further oxidation<sup>16</sup>. Similarly, stirring using excessive RPM can break the surface of the melt and trap oxides in the liquid metal. Most importantly, since Mg is highly reactive, during pouring an oxide film rapidly surrounds the liquid metal. Care must be taken to pour in a steady and even fashion so as not to

break the oxide film. If the oxide film becomes broken, it can become trapped in the final casting, leading to decreased mechanical properties<sup>69,70</sup>. Therefore, adequate mold design, effective **dross** removal and pouring technique are critical for producing high-quality Mg castings.

Fluxes and protective atmospheres are typically used to prevent oxidation of the liquid metal; however, they can also lead to unwanted inclusions<sup>2,71,72</sup>. During fluxing, if excessive material is used, unabsorbed **flux** can remain on the melt surface and become trapped in the final casting<sup>73</sup>. Some examples of flux related inclusions are MgCl<sub>2</sub>, CaCl<sub>2</sub> or FeB from boride containing fluxes. Due to these concerns, more consideration is paid to protective atmospheres for preventing melt oxidation. Some protective gases, including sulfur dioxide (SO<sub>2</sub>) and sulfur hexafluoride (SF<sub>6</sub>), modify the oxide film on the surface of the liquid metal, suppressing Mg vaporization and removing reactive gases<sup>74–76</sup>. For example, SO<sub>2</sub> can react with Mg to form MgO, MgSO<sub>4</sub> or MgS. Such compounds can enter the melt and become inclusions. As a result, adequate handling and pouring procedures should be utilized to lessen their formation. A summary of common inclusions in Mg alloys can be seen in Table 3.

The inclusion content in cast Mg alloys can be controlled and minimized by applying best practices at the foundry level. Careful selection of charge, adequate skimming of the melt, clean and moisture free equipment are some examples. Proper pouring technique and well-designed molds are also critical for minimizing entrainment of oxides due to turbulence. The use of ceramic foam and steel mesh filters can be effective in removing oxides already present in the melt and they can also control melt velocity<sup>80–82</sup>. Another method that has proven success in

**Dross:** Foreign matter such as oxides that typically form on the surface of molten metal.

**Flux:** A substance used to degas or remove oxide inclusions in a melt during casting. Fluxes typically consist of a chlorine or fluorine salt in the form of powder or as tablets.

**Morphologies:** Morphology refers to the shape, size and structure characteristics of a microstructural feature.

**Table 3:** Summary of common inclusions in Mg alloys<sup>65, 77–79</sup>

Type	Morphology	Dimensions ( $\mu\text{m}$ )	Density (g/cm <sup>3</sup> )
<i>Oxides</i>			
MgO	Particles	10–300	3.58
	Films	0.5–1 (thickness)	
		50–400 (length)	
MgO, Al <sub>2</sub> O <sub>3</sub> (spinel)	Particles		3.58
<i>Nitrides</i>			
Mg <sub>3</sub> N <sub>2</sub>	Particles	10–300	2.71
	Films	0.5–1 (thickness)	
		50–400 (length)	
<i>Carbides</i>			
Al <sub>4</sub> C <sub>3</sub>	Particles	0.1–10	2.36
CaC <sub>2</sub>	Particles	2–20	2.22
<i>Chlorides and salts</i>			
MgCl <sub>2</sub>			2.32
NaCl	Particles	10–50	2.17
CaCl <sub>2</sub>			2.15
KCl			1.98
<i>Other non-metallic inclusions</i>			
Fluorides (MgF <sub>2</sub> )			3.15
Sulfides (MgS)			2.68
Sulfates (MgSO <sub>4</sub> )			2.66
Borides (FeB)			7.15
<i>Iron-rich intermetallic compounds</i>			
Al <sub>8</sub> (Mn,Fe) <sub>5</sub> , $\alpha$ -AlMnFe, (Mn,Fe) <sub>5</sub> Si <sub>3</sub> , Al <sub>8</sub> (Mn,Fe) <sub>4</sub> RE, $\alpha$ -Fe, Fe <sub>2</sub> (Si,B), Fe <sub>3</sub> (Al,Si), (Fe,Mn) <sub>3</sub> Si	Particles, needles	< 20	4–7

removing inclusions from the liquid metal is bubbling with inert gas such as Ar or CO<sub>2</sub><sup>83</sup>. In this method, inclusions are floated to the top of melt by gas bubbles, where they can be skimmed away. Important parameters for this technique are processing time, flowrate of gas, bubble size and melt temperature<sup>83</sup>. Gas bubbling has been reported to be effective in removing smaller inclusions (< 80  $\mu\text{m}$ ), with little to no effect on inclusions larger than 800  $\mu\text{m}$ <sup>84</sup>.

It is clear that melt cleanliness is an on-going issue for Mg casting. Inclusions can be detrimental to mechanical properties. Effective control of inclusions is critical to promote the widespread use of Mg. Efforts have been made to determine best practices for foundries, ensuring high-quality castings. However, further research, especially in controlling the reaction of molten Mg with air is necessary.

## 5 Ultrasonic Processing of Lightweight Alloys

In recent years, treatment of liquid melt with high-intensity ultrasonic waves has gained significant attention by researchers. Perhaps one of the most important aspects of the application of ultrasonic waves to refine liquid metal is cavitation. Cavitation refers to the formation of cavities in the liquid metal that can become filled with dissolved gasses<sup>85</sup>. During the refinement process, these bubbles go through tensile and compression stages. Eventually, the bubbles will collapse, producing high-intensity pressure pulses, increases in temperature and high fluid velocity. Researchers have reported that the cavitation phenomenon can aid in wetting of inclusions for nucleation, removal of inclusions, melt degassing and secondary phase modification<sup>86,87</sup>.

**Degassing:** The removal of unwanted dissolved gas, typically hydrogen, from liquid metal.

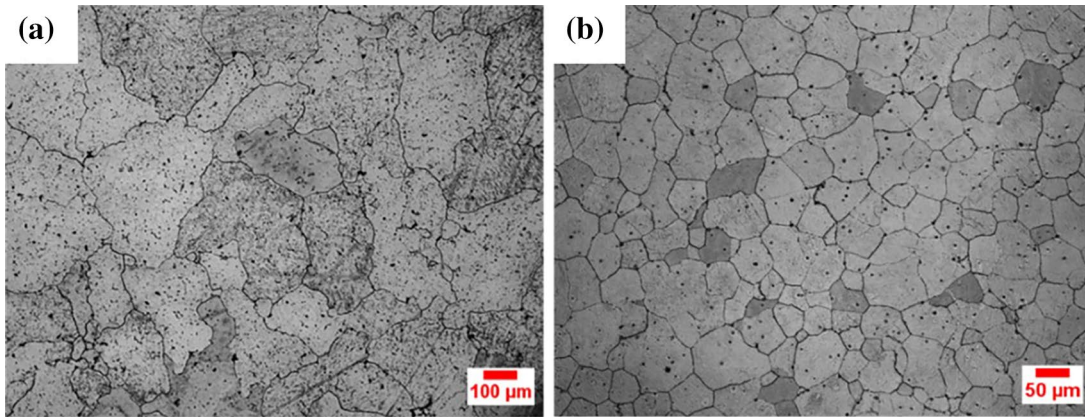


**Figure 5:** Optical micrographs showing grain structure of **a** base alloy and **b** alloy refined with 180 s of sonication<sup>91</sup>.

In addition to cavitation, streaming is also a key factor in ultrasonic processing of alloys. The sonication process can generate **hydrodynamic flows** in the liquid melt<sup>86,88,89</sup>. The flow can be represented in two forms, first are acoustic streams that stem from the pressure wave due to the vibratory motion of the sonotrode. The second form are forced convection flows occurring in the bulk fluid and near the crucible walls. The streaming process is effective in the homogenous distribution of grain refiner and reinforcement particles within the liquid metal.

A study performed by Tuan et al.<sup>90</sup>, examined the effects of sonication on an Al–Mg–Sc alloy. In their study, the effects of applying ultrasonic treatment at various melt temperatures ranging from 700 to 800 °C were examined. A 1200 W sonicator was used with a frequency of  $20.3 \pm 0.25$  kHz. The sonication was applied at 30% power and for 30 s per casting condition. Tuan et al.<sup>90</sup> determined that the temperature range of 700–740 °C was best suited for sonication. This was attributed to the shortened lifetime of cavitation bubbles at temperatures above 740 °C. As a result of sonication, the average grain size of the alloy decreased from 197 to 98 μm at a melt temperature of 720 °C. The researchers attributed the decreases in grain size to cavitation enhanced heterogeneous nucleation from ultrasonic activated particle substrates.

A recent study performed by the current authors examined the effects of varying ultrasonic time on the microstructure and mechanical properties of an **AZ91E** Mg alloy<sup>91</sup>. The authors applied the sonication treatment for 60, 120, 180 and 240 s at a frequency of 20 kHz and a vibrational amplitude of 30 μm. As a result, the grain size of the alloys was significantly refined (Fig. 5).

With 180 s of treatment time, the grain size decreased from 202 to 50 μm. The authors noted that the secondary phases of the alloy, in particular, the  $\beta$ -Mg<sub>17</sub>Al<sub>12</sub> eutectic phase and the Mn–Al-based intermetallics were also refined. As well, the mechanical properties of the refined alloys were improved. The UTS, YS and %Elongation increased from 138 MPa, 95 MPa, and 1.35% in the base alloy to 161 MPa, 111 MPa and 2.2%, respectively. The authors attributed the improvements to finer grain size, decreased Mg<sub>17</sub>Al<sub>12</sub> volume fraction and improved Mn–Al intermetallics distribution. As a result, ultrasonic treatment time was determined to have a considerable impact on the microstructure and mechanical properties of Mg alloys<sup>91</sup>.

A study performed by Srivastava and Chaudhari<sup>92</sup> examined the efficiency of sonication in dispersing nanoparticles within an Al melt. In their study, they used a **6061** Al alloy matrix reinforced with 1, 2 and 3 wt% nano-Al<sub>2</sub>O<sub>3</sub> particles. To disperse the particles, sonication was applied for 3 min. The result was uniform dispersion of Al<sub>2</sub>O<sub>3</sub> particles up to 2 wt%. The tensile strength of the composites increased while the ductility remained unchanged relative to the base alloy. Srivastava and Chaudhari determined that the addition of nanoparticles above the threshold value of 2 wt% led to poor distribution and clusters of Al<sub>2</sub>O<sub>3</sub>. Lan et al.<sup>93</sup> used ultrasonic processing as a means for the dispersion of nano-SiC particles in an AZ91D Mg alloy. The results of their study indicated a nearly uniform distribution of SiC particles within the alloy matrix. Although some agglomerates were found, the particle agglomeration was greatly reduced relative to composites prepared by mechanical stirring.

**Hydrodynamic flow:** Hydrodynamics refers to the study of liquids in motion.

**6061:** An alloy of aluminum containing 0.6% silicon, 1.0% magnesium, 0.2% chromium and 0.28% copper, by weight.

**AZ91E:** An alloy of magnesium containing 8.7% aluminum, 0.13% manganese and 0.7% zinc, by weight.

They postulated that the strong cavitation impact coupled with local high-temperature transients may have broken up the agglomerates and dispersed the particles in the melt, while at the same time, significantly enhancing their wettability.

From the available literature, it is evident that the sonication technique is largely undeveloped and requires further investigation, especially in its application to Mg alloys. Researchers have compared the effectiveness of mechanical and ultrasonic stirring; however, no attempt has been made to optimize the sonicating process with respect to the alloy and grain refiner characteristics. As a result, there is a significant lack of process to mechanical performance correlation. This implies that there is a need for a model to predict alloy mechanical property improvements based on sonicating parameters, such as time, depth and intensity, in addition to grain refiner particle size and addition level.

## 6 Conclusion and Way Forward

The demand for lightweighting of components is continuously increasing in the consumer electronics, aerospace and automotive industries. The transformation to electric vehicles is accelerating the need for light alloys of enhanced properties of relevance. Research is primarily focused on improving the mechanical and thermal properties of these alloys. Renewed interest in the fields of grain refinement using both potent nucleating particles and solute additions, melt cleanliness and best foundry practices, and effective ultrasonic processing is gaining impetus. Alloying, heat treatment, microstructure and porosity profoundly influence conductivity, and enable opportunities. Nonetheless, further research is required to elevate Mg and Al alloys to the level of ferrous alloys, especially for mechanical performance and efficiency. It must be emphasized that lightweight and high strength will be the buzz words of impact on humankind. Efforts will continue to promote tailored materials and processes with a sustainable future in mind.

## Publisher's Note

Springer Nature remains neutral with regard to jurisdictional claims in published maps and institutional affiliations.

## Acknowledgements

The authors would like to acknowledge the valuable contribution of the scholars whose research was used in this review. They thank the alumni and members of the Centre for Near-net-shape processing of materials for their research and stimulating discussions. The authors thank Dr. R.V. Krishnan for his excellent suggestions. The authors would also like to acknowledge the financial support of the Natural Sciences and Engineering Research Council of Canada (NSERC), through Canada Graduate Scholarships to both Mr. Payam Emadi (CGSD3 – 535728 – 2019) and Mr. Bernoulli Andilab (CGSD3 – 559982 – 2021), and research Grant RGPIN-06096.

## Funding

Natural Sciences and Engineering Research Council of Canada (NSERC).

## Declarations

## Conflict of Interest

The authors declare that they have no conflict of interest.

Received: 4 August 2021 Accepted: 28 September 2021  
Published: 20 January 2022

## References

1. Masson-Delmotte V, Zhai P, Pörtner H, Roberts D, Skea J, Shukla P, Pirani A, Moufouma-Okia W, Péan C, Pidcock R, Connors S, Matthews J, Chen Y, Zhou X, Gomis M, Lonnoy E, Maycock T, Tignor M, Waterfield T, IPCC (2018) 2018: Global Warming of 1.5 °C. An IPCC Special Report on the impacts of global warming of 1.5 °C above pre-industrial levels and related global greenhouse gas emission pathways, in the context of strengthening the global response to the threat of clim. IPCC, Geneva
2. Avedesian M, Baker H (1999) Magnesium and magnesium alloys. ASM International, Materials Park
3. StJohn D, Ma Q, Easton M, Cao P, Hildebrand Z (2005) Grain refinement of magnesium alloys. *Metall Mater Trans A* 36:1669–1679
4. Zheng R, Du JP, Gao S, Somekawa H, Ogata S, Tsuji N (2020) Transition of dominant deformation mode in bulk polycrystalline pure Mg by ultra-grain refinement down to sub-micrometer. *Acta Mater* 198:35–46
5. Perner A, Vetter J (2015) Lithium-ion batteries for hybrid electric vehicles and battery electric vehicles. Woodhead Publishing, Sawston, pp 173–190
6. Jian X, Geer T, Meek T and Han Q (2006) Effect of power ultrasound on grain refinement of magnesium

- AM60B alloy. In: TMS Annual Meeting Magnesium Technology 2006, San Antonio
7. Gao Q, Wu S, Lü S, Xiong X, Du R, An P (2017) Effects of ultrasonic vibration treatment on particles distribution of TiB<sub>2</sub> particles reinforced aluminum composites. *Mater Sci Eng A* 680:437–443
  8. Atamanenko T, Eskin D, Zhang L, Katgerman L (2010) Criteria of grain refinement induced by ultrasonic melt treatment of aluminum alloys containing Zr and Ti. *Metall Mater Trans A* 41:2056–2066
  9. Brandes A, Brook B (1992) *Smithells metals reference book*. Butterworth-Heinemann, Oxford
  10. Lide R (2001) *CRC handbook of chemistry and physics*. CRC Press, Boca Raton
  11. Flemings M (1974) *Solidification processing*. McGraw-Hill, New York
  12. Limmaneevichitr C, Eidhed W (2003) Fading mechanism of grain refinement of aluminum–silicon alloy with Al–Ti–B grain refiners. *Mater Sci Eng A* 349:197–206
  13. Schaffer P, Dahle K (2005) Settling behaviour of different grain refiners in aluminium. *Mater Sci Eng A* 413:373–378
  14. Bramfitt BL (1970) The effect of carbide and nitride additions on the heterogeneous nucleation behaviour of liquid iron. *Metall Trans* 1:1987–1995
  15. Zhang M, Kelly P, Easton M, Taylor J (2005) Crystallographic study of grain refinement in aluminum alloys using the edge-to-edge matching model. *Acta Mater* 53:1427–1438
  16. Emley E (1966) *Principles of magnesium technology*. Pergamon Press, Oxford
  17. StJohn D, Easton M and Qian M (2009) An inverse growth restriction model for predicting solidified grain size. In: 12th International conference on modeling of casting, welding, and advanced solidification processes, Vancouver, Canada
  18. Cai Y, Tan M, Shen G, Su H (2000) Microstructure and heterogeneous nucleation phenomena in cast SiC particles reinforced magnesium composite. *Mater Sci Eng A* 282:232–239
  19. Liu S, Zuo M (2011) Grain refinement of AZ91D magnesium alloy by in situ Al<sub>4</sub>C<sub>3</sub> particles. *Adv Mat Res* 306–307:429–432
  20. Huang Y, Zheng X, Liu B, Anopuo O, Hort N, Kainer K and Kim G (2010) Grain refinement of Mg–Al alloys by carbon inoculation. In: TMS annual meeting and exhibition magnesium technology symposium, Seattle, Washington, USA
  21. Huang Y, Kainer K, Hort N (2011) Mechanism of grain refinement of Mg–Al alloys by SiC inoculation. *Scr Mater* 64:793–796
  22. Easton M, Schiffl A, Yao J-Y, Kaufmann H (2006) Grain refinement of Mg–Al(–Mn) alloys by SiC additions. *Scr Mater* 55:379–382
  23. Suresh M, Srinivasan A, Pillai U, Pai B (2012) Grain refinement mechanism in Al–4B master alloy added pure Mg. *Mater Sci Forum* 710:161–166
  24. Guolong M, Guang H, Xiangfa L (2010) Grain refining efficiency of a new Al–1B–0.6C master alloy on AZ63 magnesium alloy. *J Alloys Compd* 491:165–169
  25. Liu S, Zhang Y, Han H, Li B (2009) Effect of Mg–TiB<sub>2</sub> master alloy on the grain refinement of AZ91D magnesium alloy. *J Alloys Compd* 487:202–220
  26. Watanabe Y, Gao YB, Guo JQ, Sato H, Miura S, Miura H (2013) Heterogeneous nucleation of pure magnesium on Al<sub>3</sub>Ti, TiC, TiB<sub>2</sub>, and AlB<sub>2</sub> particles. *Jpn J Appl Phys* 52:01AN04
  27. Tan Y, Ju D (2011) Effects of AlN particles and electromagnetic stirring on As-cast structure of AZ31 alloys. *Mater Sci Forum* 675–677:771–774
  28. Qian M, Cao P (2005) Discussions on grain refinement of magnesium alloys by carbon inoculation. *Scr Mater* 52:415–419
  29. Lu L, Dahle A, StJohn D (2005) Grain refinement efficiency and mechanism of aluminium carbide in Mg–Al alloys. *Scr Mater* 53:517–522
  30. Guang H, Xiangfa L, Haimin D (2008) Grain refinement of Mg–Al based alloys by a new Al–C master alloy. *J Alloys Compd* 467:202–207
  31. Yano E (2001) Effect of pure carbon powder on grain refining of cast magnesium alloys AZ91. *J Jpn Inst Light Metals* 51:599–603
  32. Kim Y, Yim C, You B (2007) Grain refining mechanism in Mg–Al base alloys with carbon addition. *Scr Mater* 57:691–694
  33. Tong X, You G, Liu Y, Long S, Liu Q (2019) Effect of C<sub>2</sub>H<sub>2</sub> as a novel gas inoculant on the microstructure and mechanical properties of as-cast AM60B magnesium alloy. *J Mater Process Technol* 271:271–283
  34. Reprinted from *Journal of Materials Processing Technology*, 271, Tong X, You G, Liu Y, Long S and Liu Q (2019) Effect of C<sub>2</sub>H<sub>2</sub> as a novel gas inoculant on the microstructure and mechanical properties of as-cast AM60B magnesium alloy, 271–283, Copyright (2019), with permission from Elsevier
  35. Emadi P, Rinaldi M, Ravindran C (2021) Grain refinement and fading behavior of MgB<sub>2</sub>-inoculated magnesium. *Metallogr Microstruct Anal* 10:367–376. <https://doi.org/10.1007/s13632-021-00755-5>
  36. Klösch G, McKay B, Schumacher P (2016) Preliminary investigation on the grain refinement behavior of ZrB<sub>2</sub> particles in Mg–Al alloys. Springer, Cham
  37. Sahoo S, Sahoo B, Panigrahi S (2020) Effect of in-situ sub-micron sized TiB<sub>2</sub> reinforcement on microstructure and mechanical properties in ZE41 magnesium matrix composites. *Mater Sci Eng A* 773:138883
  38. Elsayed A, Ravindran C (2011) Effect of aluminum-titanium-boron based grain refiners on AZ91E magnesium alloy grain size and microstructure. *Int J Metalcast* 5:29–41

39. Wang S, Huang Y, Yang L, Zeng Y, Hu Y, Zhang X, Sun Q, Shi S, Meng G, Hort N (2021) Microstructure and mechanical properties of Mg-3Sn-1Ca reinforced with AlN nano-particles. *J Magnesium Alloys*. <https://doi.org/10.1016/j.jma.2021.04.002>
40. Qiu W, Liu Z, Yu R, Chen J, Ren Y, He J, Li W, Li C (2019) Utilization of VN particles for grain refinement and mechanical properties of AZ31 magnesium alloy. *J Alloys Compd* 781:1150–1158
41. Seetharaman S, Subramanian J, Tun K, Hamouda A, Gupta M (2013) Synthesis and characterization of nano boron nitride reinforced magnesium composites produced by the microwave sintering method. *Materials* 6:1940–1955
42. Gupta M, Wong WLE (2015) Magnesium-based nanocomposites: lightweight materials of the future. *Mater Charact* 105:30–46
43. Zhu Z, Nie K, Deng K, Han J (2020) Fabrication of biodegradable magnesium matrix composite with ultrafine grains and high strength by adding TiC nanoparticles to Mg-1.12Ca-0.84Zn-0.23Mn (at.%) alloy. *Mater Sci Eng C*. <https://doi.org/10.1016/j.msec.2019.110360>
44. Chen LY, Xu JQ, Choi H, Pozuelo M, Ma X, Bhowmick S, Yang JM, Mathaudhu S, Li XC (2015) Processing and properties of magnesium containing a dense uniform dispersion of nanoparticles. *Nature* 528:539–543
45. Easton M, StJohn D (1999) Grain refinement of aluminum alloys: Part I. The nucleant and solute paradigms—a review of the literature. *Metall Mater Trans A* 30:1613–1623
46. Reprinted from *Journal of Alloys and Compounds*, 619, Ali Y, Qiu D, Jiang B, Pan F and Zhang MX (2015) Current research progress in grain refinement of cast magnesium alloys: a review article, 639–651, Copyright (2015), with permission from Elsevier
47. Ali Y, Qiu D, Jiang B, Pan F, Zhang MX (2015) Current research progress in grain refinement of cast magnesium alloys: a review article. *J Alloys Compd* 619:639–651
48. Wang Y, Zeng X, Ding W, Luo AA, Sachdev AK (2007) Grain refinement of AZ31 magnesium alloy by titanium and low-frequency electromagnetic casting. *Metall Mater Trans A* 38:1358–1366
49. Joshi U, Babu NH (2017) The grain refinement potency of bismuth in magnesium. *J Alloys Compd* 695:971–975
50. Guangyin Y, Yangshan S, Wenjiang D (2001) Effects of bismuth and antimony additions on the microstructure and mechanical properties of AZ91 magnesium alloy. *Mater Sci Eng A* 308:38–44
51. Zhang Y, Huang X, Li Y, Ma Z, Ma Y, Hao Y (2017) Effects of samarium addition on as-cast microstructure, grain refinement and mechanical properties of Mg-6Zn-0.4Zr magnesium alloy. *J Rare Earths* 35:494–502
52. Mulazimoglu M, Drew R, Gruzleski J (1989) Electrical conductivity of aluminium-rich Al-Si-Mg alloys. *J Mater Sci Lett* 8:297–300
53. Vandersluis E, Emadi P, Andilab B, Ravindran C (2020) The role of silicon morphology in the electrical conductivity and mechanical properties of As-cast B319 aluminum alloy. *Metall Mater Trans A* 51A:1874–1886
54. Vázquez-López C, Calderón A, Rodríguez ME, Velasco E, Cano S, Colás R, Valtierra S (2000) Influence of dendrite arm spacing on the thermal conductivity of an aluminum-silicon casting alloy. *J Mater Res* 15:85–91
55. Argo D, Drew R, Gruzleski J (1987) A simple electrical conductivity technique for measurement of modification and dendrite arm spacing in Al-Si alloys. *AFS Trans* 95:455–464
56. Narayanprabhu K, Ravishankar B (2003) Effect of modification melt treatment on casting/chill interfacial heat transfer and electrical conductivity of Al-13% Si alloy. *Mater Sci Eng A* 360:293–298
57. Sjölander E, Seifeddine S (2010) The heat treatment of Al-Si-Cu-Mg casting alloys. *J Mater Process Technol* 210:1249–1259
58. Wang R, Lu W (2013) Spheroidization of eutectic silicon in direct-electrolytic Al-Si alloy. *Metall Mater Trans A* 44:2799–2809
59. Vandersluis E, Ravindran C (2020) Effects of solution heat treatment time on the as-quenched microstructure, hardness and electrical conductivity of B319 aluminum alloy. *J Alloys Compd* 838:155577
60. Vandersluis E, Ravindran C, Bamberger M (2021) Mechanisms affecting hardness and electrical conductivity in artificially-aged B319 aluminum alloy. *J Alloys Compd* 867:159121
61. Reprinted from *Journal of Alloys and Compounds*, 867, Vandersluis E, Ravindran C and Bamberger M (2021) Mechanisms affecting hardness and electrical conductivity in artificially-aged B319 aluminum alloy, 159121, Copyright (2021), with permission from Elsevier
62. Ramirez AM, Beltrán FE, Yáñez-Limón JM, Vorobiev YV, Gonzalez-Hernandez J, Hallen JM (1999) Effects of porosity on the thermal properties of a 380-aluminum alloy. *J Mater Res* 14:3901–3906
63. Vandersluis E, Ravindran C (2019) The role of porosity in reducing the thermal conductivity of B319 Al alloy with decreasing solidification rate. *JOM* 71:2072–2077
64. Davis J (1993) *Aluminum and aluminum alloys*. ASM International, Materials Park
65. Sin SL, Elsayed A, Ravindran C (2013) Inclusions in magnesium and its alloys: a review. *Int Mater Rev* 58:419–436
66. Hu H, Luo A (1996) Inclusions in molten magnesium and potential assessment techniques. *JOM* 48:47–51
67. Bakke P and Karlsen DO (1997) Inclusion assessment in magnesium and magnesium base alloys. In: *Proc. 1997 SAE Int. Cong. & Expo., Detroit*
68. Reprinted from *Magnesium Technology 2000*, Tartaglia JM and Grebetz JC (2000) Observation of Intermetallic Particle and Inclusions Distributions in Magnesium Alloys, 113–122, Copyright (2000), with permission from Wiley

69. Griffiths W, Lai N (2007) Double oxide film defects in cast magnesium alloy. *Metall Mater Trans A* 38:190–196
70. Mirak AR, Divandari M, Boutorabi SMA, Taylor JA (2012) Effect of oxide film defects generated during mould filling on mechanical strength and reliability of magnesium alloy castings (AZ91). *Int J Cast Met Res* 25:188–194
71. Cashion S, Ricketts N, Hayes P (2002) The mechanism of protection of molten magnesium by cover gas mixtures containing sulphur hexafluoride. *J Light Met* 2:43–47
72. Cashion S, Ricketts N, Hayes P (2002) Characterisation of protective surface films formed on molten magnesium protected by air/SF<sub>6</sub> atmospheres. *J Light Met* 2:37–42
73. Friedrich HE, Mordike BL (2006) *Magnesium technology*. Springer-Verlag, Berlin
74. Chen H, Liu J, Huang W (2006) Oxidation behavior of molten magnesium in air/HFC-134a atmospheres. *J Mater Sci* 41:8017–8024
75. Ha W, Kim Y (2006) Effects of cover gases on melt protection of Mg alloys. *J Alloys Compd* 28:208–213
76. Xiong S, Liu X (2007) Microstructure, composition, and depth analysis of surface films formed on molten AZ91D alloy under protection of SF<sub>6</sub> mixtures. *Metall Mater Trans A* 38:428–434
77. Ditzel A, Scharf C (2008) *Recycling of magnesium*. Papierflieger Verlag, Clausthal-Zellerfeld
78. Oymo D, Karlsen DO, Pinfeld PMD, Mellerud T, Lie O (1994) Particle removal in pure magnesium. *Light metals* 1994:1017–1024
79. Inclusions in magnesium and its alloys: a review, Sin SL, Elsayed A and Ravindran C, *International Materials Reviews*, copyright © 2013 Institute of Materials, Minerals and Mining and ASM International, reprinted by permission of Informa UK Limited, trading as Taylor & Francis Group, [www.tandfonline.com](http://www.tandfonline.com) on behalf of Institute of Materials, Minerals and Mining and ASM International
80. Bakke P, Engh TA, Bathen E, Oymo D, Nordmark A (1994) Magnesium filtration with ceramic foam filters and subsequent quantitative microscopy of the filters. *Mater Manuf Processes* 9:111–138
81. Le C, Zhang ZQ, Cui JZ, Chang SW (2009) Study on the filtering purification of AZ91 magnesium alloy. *Mater Sci Forum* 610–613:754–757
82. Wang J, Zhou J, Tong W, Yang Y (2010) Effect of purification treatment on properties of Mg-Gd-Y-Zr alloy. *Trans Nonferrous Met Soc China* 20:1235–1239
83. Yim CD, Wu G, You BS (2007) Effect of gas bubbling on tensile elongation of gravity mold castings of magnesium alloy. *Mater Trans* 48:2778–2781
84. Housh S and Petrovich V (1992) Magnesium refining: a fluxless alternative. In: *Proc. 1992 SAE Int. Cong. & Expo.*, Detroit
85. Eskin GI (1998) *Ultrasonic treatment of light alloy melts*. Gordon & Breach, Amsterdam
86. Li Y, Feng H, Cao F, Chen Y, Gong L (2008) Effect of high density ultrasonic on the microstructure and refining property of Al-5Ti-0.25C grain refiner alloy. *Mater Sci Eng A* 487:518–523
87. Liu X, Osawa Y, Takamori S, Mukai T (2008) Microstructure and mechanical properties of AZ91 alloy produced with ultrasonic vibration. *Mater Sci Eng A* 487:120–123
88. Gao D, Li Z, Han Q, Zhai Q (2009) Effect of ultrasonic power on microstructure and mechanical properties of AZ91 alloy. *Mater Sci Eng A* 502:2–5
89. Zhang S, Zhao Y, Cheng X, Chen G, Dai Q (2009) High-energy ultrasonic field effects on the microstructure and mechanical behaviors of A356 alloy. *J Alloys Compd* 470:168–172
90. Tuan NQ, Puga H, Barbosa J, Pinto A (2015) Grain refinement of Al-Mg-Sc alloy by ultrasonic treatment. *Met Mater Int* 21:72–78
91. Emadi P, Ravindran C (2021) The influence of high temperature ultrasonic processing time on the microstructure and mechanical properties AZ91E magnesium alloy. *J Mater Eng Perform* 30:1188–1199
92. Srivastava N, Chaudhari G (2018) Microstructural evolution and mechanical behavior of ultrasonically synthesized Al6061-nano alumina composites. *Mater Sci Eng A* 724:199–207
93. Lan J, Yang Y, Li X (2004) Microstructure and microhardness of SiC nanoparticles reinforced magnesium composites fabricated by ultrasonic method. *Mater Sci Eng A* 386:284–290
94. Reprinted by permission from: Springer, *Journal of Materials Engineering and Performance*, The Influence of High Temperature Ultrasonic Processing Time on the Microstructure and Mechanical Properties AZ91E Magnesium Alloy, Emadi P and Ravindran C, Copyright (2021)



**Payam Emadi** is a Ph.D. candidate in the Mechanical Engineering Department at Ryerson University, Canada, under the supervision of Dr. C. Ravindran. Payam's research involves the development of high-strength and lightweight magnesium alloys

for use in the automotive and aerospace industries. Specifically, his work aims to promote uniform and finer magnesium grain structures via advanced processing methods. These include the addition of novel nucleants as well as the optimization of high-intensity ultrasonic irradiation. Payam's research is motivated by the potential to increase magnesium usage in industry, thereby improving fuel efficiency and decreasing emissions through lightweighting. Payam is a member of the Board of Trustees for ASM International.



**Bernoulli Andilab** is a Ph.D. Candidate under the supervision of Dr. Ravindran at the Centre for Near-net-shape Processing of Materials located at Ryerson University. Bernoulli's research focuses on the development of novel lightweight cast aluminum

alloys for automotive and aerospace applications. In particular, Bernoulli aims to improve the thermal conductivity

and mechanical properties of cast aluminum alloys using novel particle and alloying additions. His work will enable the increased use of lightweight and high-strength alloys in the next generation of automobiles. Bernoulli is a member of the Board of Trustees for the International Metallographic Society (IMS).



**Comondore Ravindran** is a professor of advanced materials at Ryerson University, Toronto, Canada. He is a Past President of the Canadian Academy of Engineering and ASM International. He is a fellow of many societies and has won numerous awards.

While in the industry, Dr. Ravindran had made several innovative R&D contributions in steel making and continuous casting. With his extensive experience in the metal casting industry and strong industrial relations, he established The Centre for Near-net-shape Processing of Materials at Ryerson University, where he has supervised several thesis students and has authored numerous technical papers with particular focus on light metals, efficiency and environment.